Advances in Science and Technology Research Journal

Advances in Science and Technology Research Journal, 2026, 20(10), 503–514
https://doi.org/10.12913/22998624/225694
ISSN 2299-8624, License CC-BY 4.0

Received: 2026.06.12
Accepted: 2026.07.20
Published: 2026.09.01

Effect of milling parameters on edge quality and delamination in a four-layer vacuum-bagged epoxy-glass fiber reinforced polymer laminate

Rafał Chatys[1], Łukasz Nowakowski[1], Mariusz Kłonica[2*]

[1] Faculty of Mechatronics and Machine Design, Kielce University of Technology, al. 1000-lecia P.P.7, 25-314, Kielce, Poland
[2] Faculty of Mechanical Engineering, Department of Production Engineering, Lublin University of Technology, ul. Nadbystrzycka 36, 20-618 Lublin, Poland
* Corresponding author's e-mail: m.klonica@pollub.pl

ABSTRACT

This article presents experimental results on the influence of selected contour milling parameters (spindle speed n and feed rate ft) on the edge quality of discs cut from a specific four-layer epoxy-glass laminate (GFRP). The laminate was formed using the vacuum bag method, comprising AEROGLASS glass fabric (163 g/m²) and the LH-160/H-10 resin system. Machining was carried out on a DMG DMU 50 CNC milling machine using a 3-flute uncoated Gühring 19992 VHM milling cutter with a diameter of 20 mm. For each sample, three characteristic diameters were measured: $Ø_1$ – the milling diameter (the actual dimension of the cut disc), $Ø_2$ – the diameter of the delamination zone below the edge, and $Ø_3$ – the diameter including protruding uncut and frayed fibres. The cutting tests were carried out at a constant feed rate of ft = 350 mm/min with a variable rotational speed of n = 5000–10 000 rpm (Series I) and at a constant rotational speed of n = 10 000 rpm with a variable feed rate of ft = 100–600 mm/min (Series II). In Series I, minimal delamination ($\Delta[Ø_1 - Ø_2]$ = 1.48 mm) and minimal fibre fraying ($\Delta[Ø_3 - Ø_1]$ = 1.30 mm) were observed at rotational speeds of 5000 and 10 000 rpm, respectively. In Series II, the overall tendency indicates an improvement in both indicators as feed rate increases, although the decrease is not strictly monotonic; the lowest total defect values were achieved at ft = 550–600 mm/min. For the investigated laminate-tool system, the results suggest that relatively higher feed rates may improve edge quality by reducing the duration of tool-material contact; however, this interpretation requires confirmation by temperature and force measurements.

Keywords: milling, delamination, laminate, edge quality, cutting parameters.

INTRODUCTION

Polymer matrix composites (PMC) are one of the fastest-growing groups of modern engineering materials [1, 2]. Their unique combination of high strength, corrosion resistance and the ability to tailor properties through the selection of components has meant that, over the last few decades, they have replaced traditional structural materials in many key industrial sectors, particularly in aerospace, the automotive industry, medicine and sports technology [3, 4].

Despite their excellent performance characteristics, laminated composites (laminates) present significant technological challenges during machining. The anisotropy of the structure, brittle fibre fracture and the temperature sensitivity of the polymer matrix mean that standard cutting parameters used for metals lead to the formation of characteristic defects, the most serious of which is delamination (the separation of individual layers of the laminate [5, 6]). Delamination, alongside fibre fraying, fibre pull-out and thermal burn-through of the resin, directly reduces the fatigue and static strength of finished composite components, which, in the aforementioned applications, compromises operational safety [7].

Although general recommendations for machining GFRP composites are available, there is still limited quantitative information on how spindle speed and feed rate separately affect delamination, fibre fraying and dimensional deviation in very thin, vacuum-bagged, four-layer epoxy-glass laminates. In particular, the current state of knowledge does not sufficiently describe the combined behaviour of the actual milled diameter ($Ø_1$), the delamination-zone diameter ($Ø_2$) and the fibre-envelope diameter ($Ø_3$) for laminates produced from AEROGLASS 163 g/m² fabric and the LH-160/H-10 resin system. The aim of this study is therefore to determine, for this specific material-tool-machine configuration, the effect of spindle speed n and feed rate ft on these three geometrical indicators of edge quality, and to identify machining conditions that reduce delamination and fibre fraying without worsening dimensional accuracy.

POLYMER-MATRIX COMPOSITES

As an engineering material, a composite consists of at least two components with different properties which, when combined, form a material with properties that neither component possesses on its own. According to the classical approach, the structure of a composite comprises a continuous phase (matrix), which acts as a binder, and a dispersed phase (reinforcement), which is responsible for transferring mechanical loads.

Literature [8] points out that, depending on the type of matrix, composites are divided into three main groups: those with a ceramic matrix (CMC), a metallic matrix (MMC) and a polymer matrix (PMC). Within PMC, the basic classification is based on the thermal behaviour of the matrix: thermosetting resins (epoxy, polyester, vinyl ester) undergo a single, irreversible cross-linking reaction, whilst thermoplastic resins reversibly change their plasticity under the influence of temperature. The mechanical properties of both groups are comparable, however thermosetting resins are more commonly used in structural applications due to their superior dimensional stability at elevated temperatures.

Depending on the nature of the matrix phase, composites are classified as granular, fibrous and layered (laminates). Fibrous and layered composites are of particular technical importance, as they offer the highest strength properties of all PMCs [5, 8].

Composite components

Among reinforcing components, glass fibres occupy a special position and account for approximately 85% of the tonnage of reinforcements used in PMC production, despite the rapid growth of carbon and aramid fibres. The technology for manufacturing glass fibres has been established for decades (Table 1), enabling the production of reinforcements with predictable, repeatable properties. Boron-aluminum-silicon glass fibres (type E) are primarily used to reinforce PMC; these fibres have a tensile strength of around 3500 MPa and a Young's modulus of 77 GPa [9]. Reinforcement can take the form of rovings, chopped or continuous mats, non-woven fabrics and woven fabrics. Glass fabrics are a widely used type of reinforcement due to their good drapability and their ability to be impregnated with unsaturated and epoxy resins [10, 11]. The weight of the fabrics ranges from several dozen to over 2000 g/m², which allows for extensive optimisation of the reinforcement-to-weight ratio of the finished laminate. To improve strength and corrosion resistance, ECR, S and R glass fibres, as well as quartz fibres, have been developed and are listed in Table 1. Other commercially available reinforcements, including S2 glass and basalt fibres, may also be used in polymer composites, but they were not included in Table 1 because they were not considered in the experimental part of this study [12, 13].

The matrix in GFRP composites is most commonly epoxy, polyester or vinyl ester resin. Epoxy resins – produced by the polyaddition of bisphenol and epichlorohydrin – are characterised by very good mechanical properties (R_m = 40–85 MPa, E = 2.1–5.5 GPa), low shrinkage during curing and excellent adhesion to reinforcing fibres. Their disadvantages include a relatively high price and the difficulty of impregnating dense fabrics [9].

The vacuum bag method is one of the methods used to produce laminates

The technology for manufacturing PMC laminates encompasses a range of methods, from

Table 1. Mechanical properties of selected types of glass fibres [9]

Type of glass	Density [g/cm³]	R_m [MPa]	E [GPa]	Extension [%]	$T_{softening}$ [°C]
E	2.52	3 500	77	4.8	846
ECR	2.72	4 750	86	4.8	952
S	2.49	4 585	85	5.7	1 056
R	2.50	4 750	86	4.8	952
Quartz	2.20	6 000	78	7.7	1 220

simple manual lamination to advanced RTM, VARTM, VAP and RFI processes. The works [6, 9] emphasise that the choice of moulding method decisively determines the quality of the finished composite, in particular the uniformity of the matrix distribution, the porosity and the volume fraction of the reinforcement.

The vacuum bag method combines the characteristics of hand lay-up and pressure curing (Figure 1). The vacuum created (typically -0.6 to -0.9 bar) provides mechanical pressure that bonds the laminate layers during curing, allowing trapped air and excess resin to be removed [14].

The main advantages of this technology include: improved wetting of the reinforcement [15, 16], a reduction in pores and microcracks at the interfaces between layers, a higher proportion of reinforcement in the final composite, and consequently higher strength.

The delamination mechanism during defect initiation

Delamination is one of the most serious structural defects in laminated composites, involving the separation (delamination) of adjacent layers. In their paper, the authors [9, 17] define delamination as the initiation and propagation of a crack at the layer interface, classifying it according to fracture schemes I (opening), II (in-plane shear) and III (out-of-plane shear).

During the moulding process, delamination can be caused by: trapped air or moisture between the layers, incorrect pressure or temperature during curing, cooling too quickly, which causes residual stresses, uneven resin saturation, and errors in the layering process.

Contaminants at the layer interfaces – such as fine particles, oils and moisture – reduce local adhesive bonding, creating crack initiation points. During machining, delamination is initiated by cutting forces acting perpendicular to the laminate plane.

Previous studies [18, 19] indicate that, when performing peripheral milling of laminated composites, axial and radial forces can lead to local delamination of the laminates, particularly near the machined edge. This phenomenon is strongly dependent on cutting parameters such as speed (vc), feed rate (ft) and the geometry and sharpness of the tool.

Milling of polymer-matrix composites

Milling is one of the most commonly used machining techniques for PMC composites, enabling the shaping of complex geometries with high dimensional accuracy. However, as Grzesik [20] and tool manufacturers' catalogues indicate [21], machining PMC is generally more difficult than machining homogeneous metals, due to anisotropy, a tendency towards fibre pull-out, fraying, and excessive heat generation leading to matrix degradation.

One of the factors affecting the quality of GFRP machining is the choice of cutting tool material in relation to the machining technique.

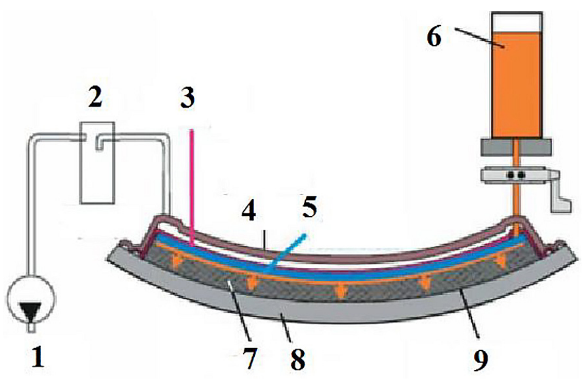

Figure 1. Vacuum bagging method for forming laminates [9]: 1 – vacuum pump; 2 – resin trap 3 – separation membrane; 4 – vacuum bag; 5 – release medium; 6 – resin; 7 – dry preform; 8 – mold; 9 – release coating

Glass fibre reinforcement has a hardness of 6–7 on the Mohs scale, which causes rapid wear of high-speed steel (HSS) tools, whilst solid carbide (VHM) tools demonstrate significantly higher durability. The use of diamond coatings DLC (Diamond-Like Carbon), CVD (Chemical Vapor Deposition) further increases tool life and reduces chip adhesion [20].

The cutting speed and feed rate (ft) must be carefully selected to minimise mechanical stresses and excessive heat generation in the machining zone. An excessively high vc may promote softening of the polymer matrix, whilst an excessively low ft may increase the contact time between the tool and the material, resulting in a rise in temperature. Optimal cooling using the minimum quantity lubrication (MQL) method minimises the penetration of fluid into the pores of the composite [20].

The optimal milling parameters for GFRP depend on the specific properties of the composite, its thickness, fibre orientation and the tool used. This paper contributes to the determination of these parameters for a specific material system, namely a 4-layer epoxy-glass laminate formed using the vacuum bag method.

MATERIALS AND METHODS

Laminate components

To carry out the task, AEROGLASS glass fabric with a weight of 163 g/m² was used as reinforcement; this fabric is characterised by good drapability, satisfactory air-release properties during the lamination process, and very good weather resistance [11]. The fabric is designed for impregnation with both polymer resins (such as polyester and epoxy).

The laminate consisted of four plies of the same glass fabric arranged in the same 0/90 fabric orientation relative to the machining coordinate system. The nominal input masses used during lay-up were 95.64 g of fabric and 125 g of resin system (86 g LH-160 + 39 g H-10), which correspond to approximate input mass fractions of 43.3 wt.% reinforcement and 56.7 wt.% resin system.

The matrix consisted of the LH-160/H-10 resin system from HAVEL Composites (Table 2). The LH-160 epoxy resin, based on bisphenol A resin, is characterised by low viscosity (0.7–0.9 Pa•s at 25 °C), very good resistance to crystallisation and a low crystallisation temperature. After curing with H-10 hardener in a weight ratio of 100:45 g, the manufacturer reports a heat stability temperature of 50 °C (curing at 25 °C, min. 2 days) or 80–90 °C (post-curing at 50–60 °C for 3 h). This catalogue parameter should not be treated as the glass transition temperature Tg; it is used only as an indicator of the temperature sensitivity of the resin system.

Manufacture of laminate using the vacuum bag method

The four-layer glass laminate was manufactured using the vacuum bag method. The moulding process involved: preparing the glass mould (degreasing – Figure 2a and waxing – Figure 2b), cutting out 4 layers of glass fabric with a total weight of 95.64 g, mixing the resin system (86 g of resin + 39 g of hardener), impregnating successive layers of fabric and laying them on the mould, applying peel ply, a vacuum mat and PRO-VAC 100-LB-75 perforated film (Figure 2c), sealing the vacuum bag with butyl tape and connecting the vacuum pump to create a vacuum of -0.6 bar. The vacuum was maintained for 30 minutes during compaction and air removal, and was not maintained throughout the full curing period. Curing took place at room temperature (23 °C) for a minimum of 48 hours. The measured thickness of the cut blanks (workpieces) ranged from 0.79 to 1.00 mm.

Table 2. Technical specifications of the resin system LH-160/H-10 [8]

Property	Value
Heat stability temperature (25 °C / 2 days)	50 °C
Heat stability temperature (50–60 °C / 3 hours)	80–90 °C
Viscosity at 25 °C	0.7–0.9 Pa·s
Weight ratio of LH-160 to H-10	100 : 45 g
Pot life at 25°C (ratio 100:45)	20–25 min

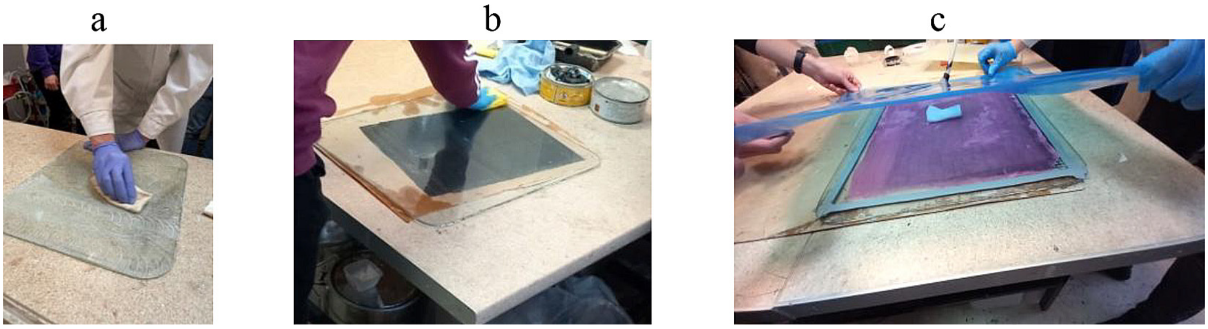

Figure 2. Degreasing (a) and waxing (b) of the mould with release materials in place (peel ply, vacuum mat and perforated film)

Workpiece and cutting tool

The selection of the machine tool and the machining method used for sample preparation is a crucial issue [22–24]. The machining was carried out on a DMG DMU 50 CNC milling machine – a 5-axis milling machine controlled numerically (Heidenhain iTNC 530 controller), which features a positioning accuracy of ±0.01 mm, a maximum spindle speed of 10,000 rpm and a drive power of 9/13 kW.

A 3-flute uncoated Gühring 19992 solid carbide end mill with a diameter of 20 mm, a 45° helix angle, a cutting edge length of 38 mm and a total length of 104 mm was used for the machining. The tool material hardness was 90–94 HRA. The workpiece were clamped in a special holder enabling repeatable and rigid clamping on the machine tool table (Figure 3). Before the tests, the cutter was visually inspected to exclude visible edge chipping. Tool wear was not measured quantitatively during the experiment (e.g. flank wear VB or cutting-edge radius).

Research plan and scope

The tests were carried out in two series. In Series I, a constant feed rate of ft = 350 mm/min was maintained, and the spindle speed n was varied within the range of 5000–10,000 rpm (in 500 rpm increments). In Series II, a constant rotational speed of n = 10.000 rpm was maintained and the feed rate ft was varied within the range of 100–600 mm/min (in 50 mm/min increments).

The entry into the material involved moving in a straight line at a defined entry depth (Z = -5 mm at a feed rate of 5000 mm/min), followed by an approach to the workpiece along an arc tangent to the first section of the tool path in the material, in line with the machining direction (Figure 4).

A total of 22 discs with a nominal diameter of 52 mm were cut from the laminate. For each sample, three characteristic diameters ($Ø_1$, $Ø_2$ and $Ø_3$) were identified, and each diameter was measured on optical/digital images of the disc edge; the mean value was then used in the analysis. The assessment of edge quality was based

Figure 3. View of the workpiece secured to the table of the DMU 50 machine tool using a special clamp

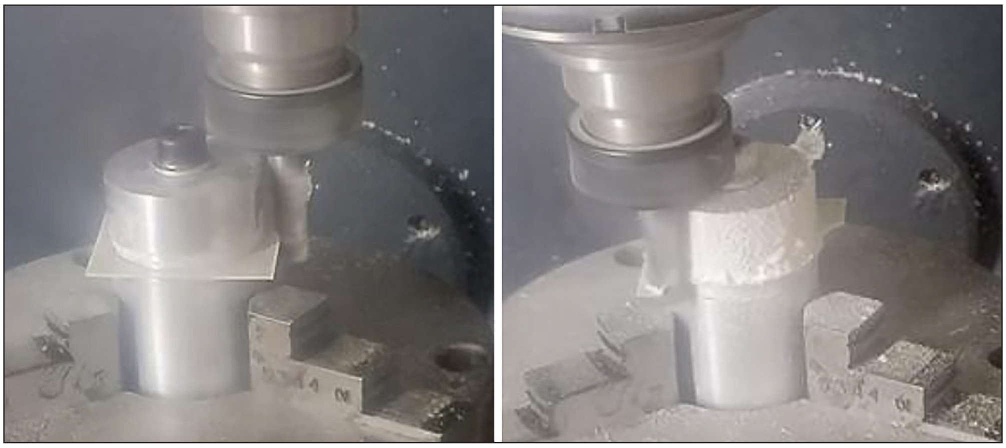

Figure 4. Machining along the tangent arc of the tool path in material aligned with the machining direction

on these geometrical measurements, whereas visual observation was used only to identify the type of defect, such as burrs, fraying, fibre pull-out and delamination.

RESULTS AND DISCUSSION

The effect of spindle speed on edge quality

In Series I, at a constant feed rate of f_t = 350 mm/min, measurements were taken of three characteristic diameters for each sample (Figure 5): $Ø_1$ (milling diameter), $Ø_2$ (diameter of the delamination zone) and $Ø_3$ (diameter encompassing the protruding, uncut glass fibres).

Based on the measurements, the following edge quality indices were calculated: $\Delta[Ø_1-Ø_2]$ – a measure of the depth of the delamination zone (a lower value = less delamination), and $\Delta[Ø_3-Ø_1]$ – a measure of the extent of fibre fraying (lower value = fewer protruding fibres). The results are summarised in Table 3.

Quantitative measurements reveal a complex relationship between rotational speed and two distinct damage indices. The delamination index $\Delta[Ø_1-Ø_2]$ reaches a minimum value of 1.48 mm at n = 5000 rpm, whilst the maximum value of 3.15 mm is observed at n = 9500 rpm. The fibre fraying index $\Delta[Ø_3-Ø_1]$, on the other hand, is smallest and therefore most favourable at n = 10,000 rpm (1.30 mm), and largest at n = 8500 rpm (3.43 mm).

The sum of both indicators, taken as a measure of total edge damage, takes the following values: 2.87 mm at n = 10,000 rpm (best), 3.92 mm at n = 8000 rpm, and 5.53 mm at n = 8500 rpm (worst). The result at n = 9500 rpm ($\Delta[Ø_1-Ø_2]$ = 3.15 mm) should be treated as an anomaly that may be associated with unfavourable dynamic conditions of the machine tool-holder-workpiece-tool system; however, this explanation cannot be confirmed without vibration or force measurements.

The results indicate that n = 10,000 rpm minimises fibre fraying, as a higher cutting speed reduces the contact time between the blade and an individual fibre, promoting a clean cut rather than tearing. At the same time, n = 5000 rpm results in the least delamination, as a lower speed is associated with a higher feed per tooth at a constant feed rate, which limits the duration of heat generation in the cutting zone.

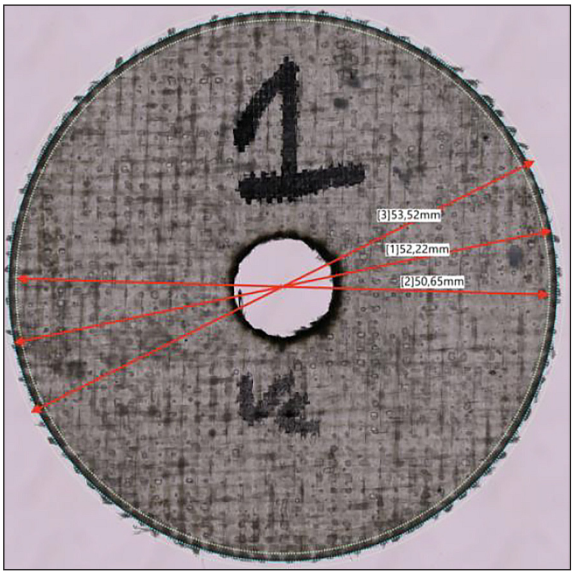

Figure 5. Milling finish of the edges of a 4-layer laminate at a spindle speed n of 10,000 rpm and a constant feed rate of f_t = 350 mm/min

Table 3. The effect of rotational speed n on edge quality at a constant f_t = 350 mm/min

n [rpm]	$Ø_1$ milling [mm]	$Ø_2$ delamination [mm]	$Ø_3$ fibres [mm]	$Δ[Ø_1–Ø_2]$ [mm]	$Δ[Ø_3–Ø_1]$ [mm]
10000	52.22	50.65	53.52	1.57	1.30
9500	52.26	49.11	54.51	3.15	2.25
9000	52.24	50.75	55.31	1.49	3.07
8500	52.27	50.17	55.70	2.10	3.43
8000	52.23	50.58	54.50	1.65	2.27
7500	52.27	50.25	54.91	2.02	2.64
7000	52.25	50.74	55.07	1.51	2.82
6500	52.33	50.67	55.45	1.66	3.12
6000	52.27	50.50	55.47	1.77	3.20
5500	52.25	50.49	54.78	1.76	2.53
5000	52.26	50.78	55.46	1.48	3.20

The results confirm the observations of Grzesik [20], who emphasises that, in the case of materials with low thermal conductivity, minimising the duration of thermal exposure is crucial. However, within the range studied, there is no clear-cut optimal rotational speed, the selection of which depends on the priority (minimising delamination versus minimising fibre fraying). In terms of the overall assessment of edge defects, n = 10,000 rpm proves to be the most favourable, which contrasts with the initial visual quality assessments indicating n = 5000–5500 rpm.

The effect of feed rate on edge quality

In Series II, at a constant rotational speed of n = 10,000 rpm, the effect of a variable feed rate (f_t) on three characteristic disc diameters was investigated: $Ø_1$ (milling), $Ø_2$ (delamination zone) and $Ø_3$ (fibre reach). The results, together with the calculated indices $Δ[Ø_1–Ø_2]$ and $Δ[Ø_3–Ø_1]$, are summarised in Table 4.

Quantitative measurements in Series II reveal an overall downward tendency in edge damage with increasing feed rate, but the relationship is not strictly monotonic. The delamination index reaches a maximum of 2.15 mm at ft = 350 mm/min and a minimum of 1.01 mm at ft = 600 mm/min. The fibre fraying index is highest (2.77 mm) at ft = 200 mm/min and lowest (1.30 mm) at ft = 500 mm/min. The total defect measure decreases from 4.24 mm at ft = 100 mm/min to 2.45 mm at ft = 600 mm/min, although local increases at ft = 250 and 300 mm/min interrupt strict monotonicity. This behaviour is therefore interpreted as a trend supported by the trend line in Figure 9, rather than as a strictly monotonic decrease.

Within the investigated range, the results suggest that a higher feed rate can reduce edge damage for the tested laminate-tool configuration. This conclusion should not be generalised to all GFRP laminates without additional tests involving other laminate thicknesses, tools and cooling/lubrication conditions.

A possible explanation for the observed improvement at higher feed rates is the increase in chip thickness and the reduction in the time of contact between the cutting edge and the material. This may reduce the duration of frictional heating; however, because temperature was not measured in the present work, the thermal interpretation should be treated as a hypothesis requiring further experimental verification.

Because the manufacturer reports a heat stability temperature of 50 °C for the LH-160/H-10 system cured at 25 °C, the matrix may be sensitive to temperature increases during machining. This parameter is not equivalent to Tg and is used here only as a catalogue-based indicator of thermal sensitivity. At ft = 350 mm/min, the delamination index is highest (2.15 mm), which may result from unfavourable dynamic or thermal conditions, but this cannot be confirmed without temperature, force or vibration measurements.

The results are consistent with the mechanism described by [6, 7]: at a very low feed rate (f_t = 100 mm/min), each blade repeatedly rubs against the same surface rather than cutting through it, causing the friction effect to increase heat and promote fibre tearing rather than a clean cut.

Table 4. The effect of the feed rate (ft) on edge quality at a constant n = 10,000 rpm

f_t [mm/min]	$Ø_1$ milling [mm]	$Ø_2$ delamination [mm]	$Ø_3$ fibres [mm]	$Δ[Ø_1−Ø_2]$ [mm]	$Δ[Ø_3−Ø_1]$ [mm]
100	52.47	50.67	54.91	1.80	2.44
150	52.52	50.93	54.89	1.59	2.37
200	52.37	51.34	55.14	1.03	2.77
250	52.34	50.64	54.75	1.70	2.41
300	52.33	50.84	54.82	1.49	2.49
350	52.43	50.28	53.99	2.15	1.56
400	52.26	50.73	53.97	1.53	1.71
450	52.32	50.71	53.74	1.61	1.42
500	52.28	50.57	53.58	1.71	1.30
550	52.24	50.89	53.85	1.35	1.61
600	52.29	51.28	53.73	1.01	1.44

Delamination, i.e. the local separation of layers, manifests as bright lines and blisters at the edge, caused by crack initiation at the interface between layers. In the present study, the observed defects may result from a combined influence of mechanical loading and local heating. At low feed rates (ft = 100–200 mm/min), the longer tool-material contact time may promote rubbing and fibre tearing, but the relative contribution of thermal and mechanical effects cannot be separated because temperature and cutting forces were not recorded.

Edge quality assessment

In order to standardise and quantify the assessment of the quality of the edges of the cut discs, a scoring system on a scale of 1–5 was developed. The method is based solely on data obtained from microscopic measurements, i.e. from three measured diameters: $Ø_1$ (milling), $Ø_2$ (delamination zone) and $Ø_3$ (fibre envelope) – without any subjective input from the observer.

For each sample, three partial scores were assigned on a scale of 1 to 5, and the overall score Q was then calculated as their weighted average:

$$Q = 0.40 \cdot S\text{-}del + 0.40 \cdot S\text{-}fray + 0.20 \cdot S\text{-}dim \tag{1}$$

where: *S-del* – the delamination score (weight 40%), *S-fray* – the fibre-fraying score (weight 40%), and *S-dim* – the dimensional-accuracy score (weight 20%).

The weights and threshold values in Table 5 were adopted as an engineering, diameter-based assessment criterion for this preliminary study. They were not taken from a dedicated standard, because no standardised scoring method based simultaneously on $Ø_1$, $Ø_2$ and $Ø_3$ was identified for such thin GFRP discs. Higher weights were assigned to S-del and S-fray because they describe structural edge defects, whereas the lower weight of S-dim reflects dimensional deviation, which mainly results from elastic springback and does not directly describe interlaminar damage.

Figures 6 and 7 show the results of the scoring assessment for both test series. The bars represent the values of the three partial scores, whilst the solid line represents the total score Q, calculated using the formula provided. Figures 8 and 9 show the direct measurement indices: $Δ[Ø_1−Ø_2]$ (width of the delamination zone)

Table 5. Sub-score ranges S-del, S-fray and S-dim — classification criteria and thresholds adopted in this study

Assessment	S-del: $Δ[Ø_1−Ø_2]$ [mm]	S-fray: $Δ[Ø_3−Ø_1]$ [mm]	S-dim: $|Ø_1 − 52.00|$ [mm]
5	≤ 1.50	≤ 1.50	≤ 0.25
4	1.51–1.80	1.51–2.00	0.26–0.33
3	1.81–2.20	2.01–2.50	0.34–0.42
2	2.21–2.80	2.51–3.00	0.43–0.50
1	> 2.80	> 3.00	> 0.50

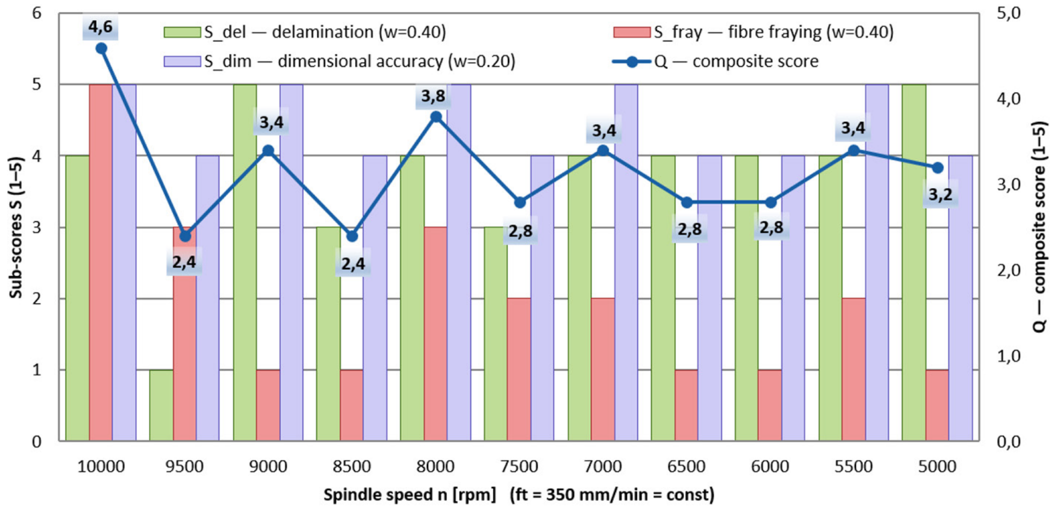

Figure 6. Partial ratings S_del, S_fray, S_dim and total rating Q — Series I (variable rotational speed n, ft = 350 mm/min = const)

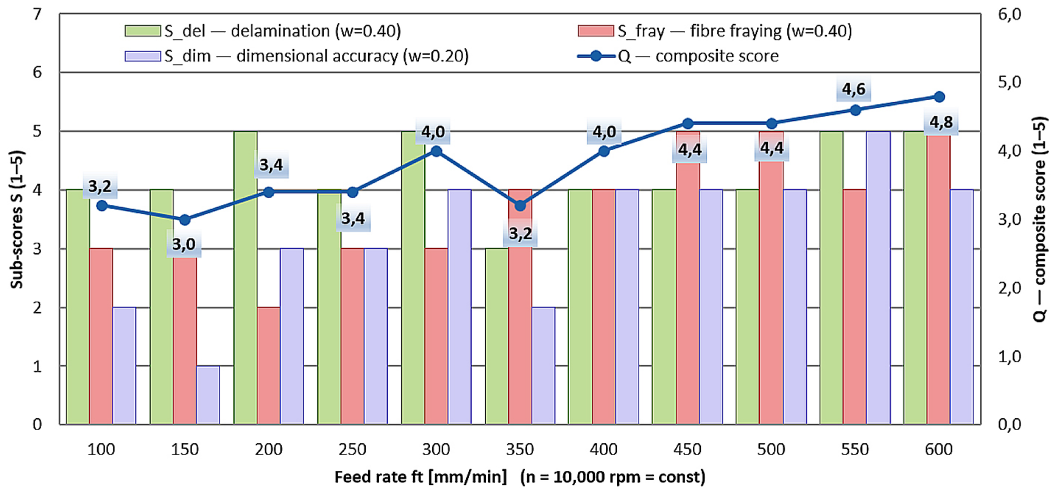

Figure 7. Partial scores S-del, S-fray, S-dim and the total score Q — Series II (variable feed rate ft, n = 10.000 rpm = const)

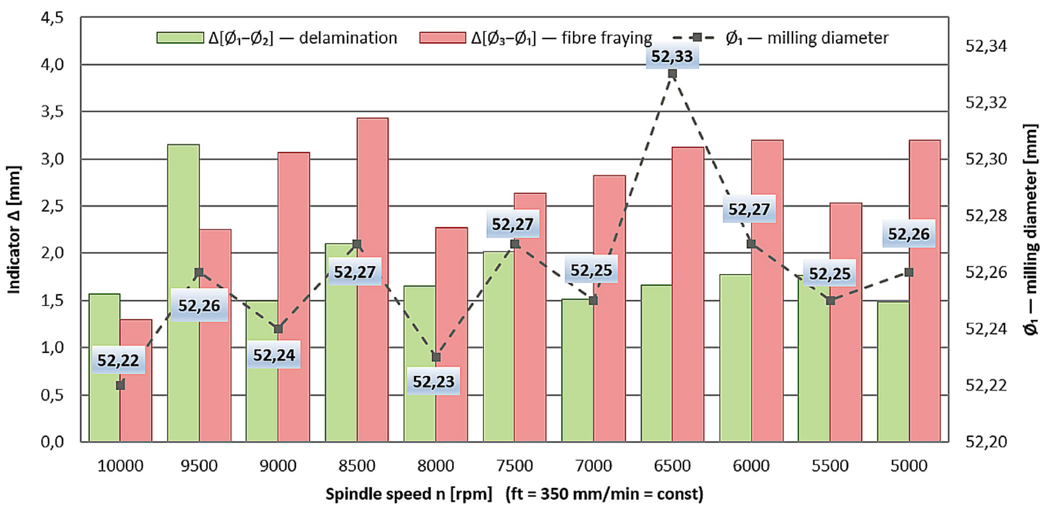

Figure 8. Delamination indices $\Delta[Ø_1–Ø_2]$ and fibre fraying indices $\Delta[Ø_3–Ø_1]$, and milling diameter $Ø_1$ — Series I (variable n)

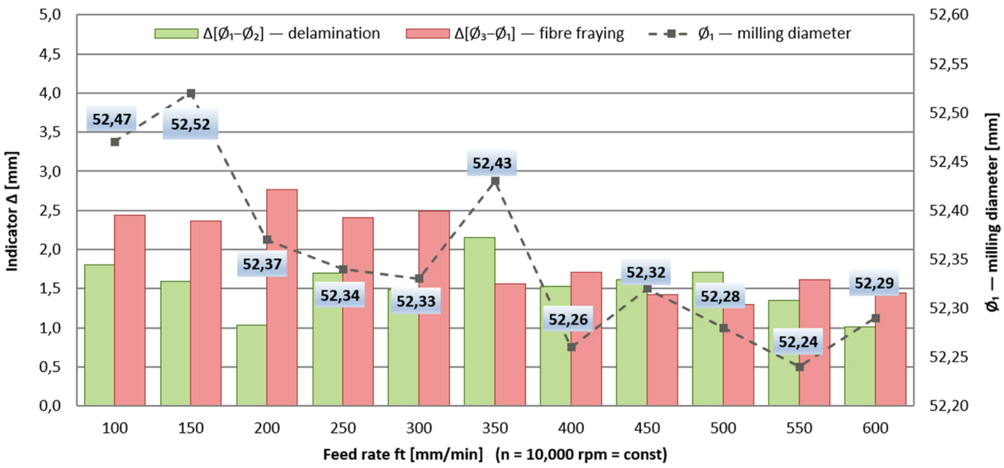

Figure 9. Delamination indices Δ[Ø₁–Ø₂] and fibre fraying indices Δ[Ø₃–Ø₁], and milling diameter Ø₁ — Series II (variable f_t)

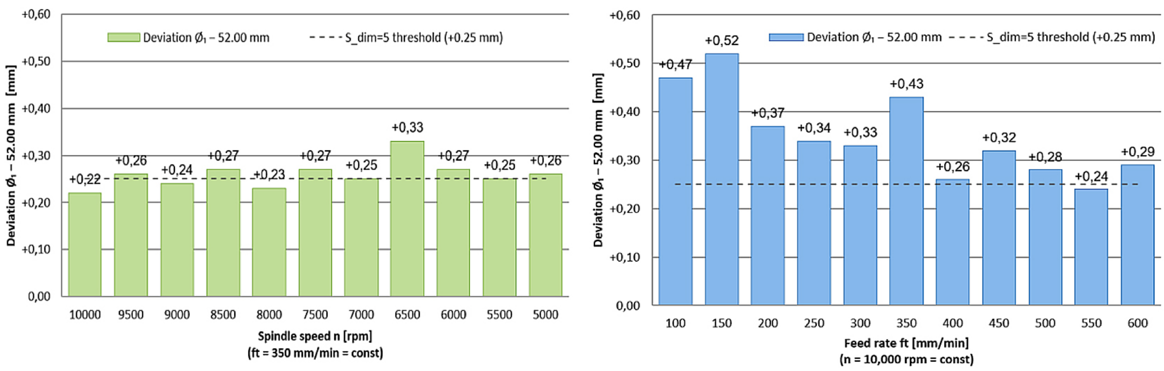

Figure 10. Deviation of the measured milling diameter Ø₁ from the nominal dimension of 52.00 mm (CNC milling: Ø = 52.00 mm) — Series I (n = 5000–10,000 rpm, ft = 350 mm/min = const) and Series II (ft = 100–600 mm/min, n = 10,000 rpm = const). Dark colour: deviation > +0.25 mm. Dashed line: threshold S_dim = 5. Solid line in series II: linear regression (r = −0.826)

and Δ[Ø₃–Ø₁] (extent of fibre fraying), together with the measured milling diameter Ø₁.

Analysis of dimensional accuracy

A dimensional analysis of Ø₁ (milling diameter) revealed high process stability: in Series I, the Ø₁ values range from 52.22 to 52.33 mm (deviations from the nominal value of 52 mm: +0.22 to +0.33 mm), with a range of just 0.11 mm. In series II, Ø₁ ranges from 52.24 to 52.52 mm (deviations of +0.24 to +0.52 mm), with a range of 0.28 mm. Constant positive deviations of the Ø₁ dimension from the nominal value (52 mm) indicate the effect of material springback following the passage of the cutting edge – a phenomenon characteristic of PMC, where the bending fibres push the tool out of the cutting path. The greatest springback was observed at ft = 150 mm/min (Ø₁ = 52.52 mm, deviation +0.52 mm), and the smallest at ft = 550 mm/min (Ø₁ = 52.24 mm, deviation +0.24 mm). This confirms that a higher feed rate not only reduces edge damage but also improves the dimensional accuracy of the cut disc.

In Series I (variable rotational speed n, feed rate ft = 350 mm/min = constant), the deviations in Ø₁ − 52.00 mm are small and highly stable: they range from +0.22 mm (n = 10,000 rpm) to +0.33 mm (n = 6500 rpm) with a standard deviation σ = 0.027 mm. The criterion S_dim = 5 (deviation ≤ 0.25 mm) was met for five spindle speeds: 10,000, 9000, 8000, 7000 and 5500 rpm. The stability of the deviation indicates that a change in rotational speed within the range of 5000–10,000 rpm does not significantly affect the elastic rebound effect at a constant feed rate.

In Series II (variable feed rate ft, n = 10,000 rpm = const), the deviations show a stronger dependence on the feed rate: from +0.24 mm (ft

= 550 mm/min) to +0.52 mm (ft = 150 mm/min), with σ = 0.085 mm – more than three times higher than in Series I. Pearson's correlation coefficient r = −0.826 confirms a negative correlation: a higher feed rate generally reduces springback. Only one sample, ft = 550 mm/min, met the criterion S_dim = 5 (deviation ≤ 0.25 mm). The remaining high-feed samples were close to this threshold but did not formally meet it.

Figure 10 shows a graphical comparison of the deviations for both series, with enlarged labels, the S_dim = 5 threshold line (+0.25 mm) and the linear trend line for Series II.

CONCLUSIONS

Based on the experimental studies conducted on the cylindrical milling of a 4-layer epoxy-glass laminate, the following conclusions can be drawn:

1. Spindle speed has a different effect on the two indicators of edge damage. Minimum delamination ($\Delta[Ø_1–Ø_2]$ = 1.48 mm) was achieved at n = 5.000 rpm, whilst minimum fibre fraying ($\Delta[Ø_3–Ø_1]$ = 1.30 mm) was achieved at n = 10,000 rpm. In terms of the total defect measure (the sum of both indices), the most favourable speed in the tested range is n = 10,000 rpm (sum 2.87 mm), and the least favourable is n = 8500 rpm (sum 5.53 mm). The result at n = 9500 rpm may indicate unfavourable dynamic conditions, but this requires confirmation by vibration or force measurements.
2. The feed rate shows a generally beneficial influence on edge quality in the tested range, but the decrease in total damage is not strictly monotonic. The best result was obtained at ft = 600 mm/min, with minimum delamination ($\Delta[Ø_1–Ø_2]$ = 1.01 mm) and the lowest total defect measure (2.45 mm). These results suggest that, for the investigated laminate and tool, a relatively short tool-material contact time may be more important than the use of very low feed rates; however, this conclusion should be verified for other laminate systems and cutting tools.
3. The observed edge degradation may be related to both mechanical loading and local heating of the epoxy matrix. Because temperature, cutting forces and vibration were not measured, the thermal-softening mechanism should be treated as a plausible explanation rather than a directly confirmed phenomenon. The manufacturer's heat stability temperature of the LH-160/H-10 system is not equivalent to Tg and was used only as an indicator of matrix thermal sensitivity.
4. A 3-flute uncoated solid carbide end mill (Gühring 19992, Ø 20 mm) was used in all tests. The high hardness of cemented carbide (90–94 HRA) and sharp cutting edges are advantageous for machining abrasive glass-fibre laminates.
5. Based on quantitative measurements of three characteristic diameters, the recommended parameters for the tested GFRP laminate (163 g/m^2 glass fabric, LH-160/H-10 resin) and the uncoated Gühring 19992 solid carbide milling cutter (Ø 20 mm) are ft = 550–600 mm/min at n = 10.000 rpm. This range provides low delamination ($\Delta[Ø_1–Ø_2] \approx$ 1.01–1.35 mm), low fibre fraying ($\Delta[Ø_3–Ø_1] \approx$ 1.44–1.61 mm) and favourable dimensional accuracy. If minimising fibre fraying alone is the priority, n = 10,000 rpm at ft = 350 mm/min remains a favourable setting ($\Delta[Ø_3–Ø_1]$ = 1.30 mm), but it does not provide the lowest delamination index.
6. The study should be treated as preliminary and limited to one laminate architecture, one cutting tool and one nominal cutting depth. The main limitations are the lack of repeated machining trials for each parameter set, the absence of direct temperature, force and vibration measurements, the lack of quantitative tool-wear monitoring, and the absence of roughness measurements and industrial validation. Future work should include cutting-depth variation, cooling/lubrication strategies, tool-wear analysis and validation on industrial laminate components.

REFERENCES

1. Mortennsen A. Concise Encyclopedia of Composite Material, Publ. ELSEVIER, Singapur - London-New York, 2007.
2. Gibson Ronald F. Principles of Composite Material Mechanics, Publ. CRC Press, Taylor&Francis Group, Boca Ration-London-New York, 2007.
3. Bielawski R., Rządkowski W., Kowalik M. P., Kłonica M. Safety of aircraft structures in the context of composite element connection. International Review of Aerospace Engineering (IREASE). 2020; 13: 159–164. https://doi.org/10.15866/irease.v13i5.18805
4. Rech J., Grzesik W. New trends in hybrid finishing

processes of metallic additively fabricated parts – A short review. Journal of Machine Engineering, 2023; 23: 36–46. https://doi.org/10.36897/jme/162284

5. Nowakowski L., Bronis M., Blasiak S., Skrzyniarz M. A method for determining the minimum thickness of the cut layer in precision milling. Materials 2025; 18: 189. https://doi.org/10.3390/ma18010189
6. Ciecieląg K., Wiertel M., Zaleski R. Microstructural analysis of glass and carbon fiber-reinforced epoxy composites using positron annihilation lifetime spectroscopy: effects of machining and temperaturę. Composites Part A: Applied Science and Manufacturing. 2026; 206. https://doi.org/10.1016/j.compositesa.2026.109810
7. Nowakowski L., Blasiak S., Skrzyniarz M. Influence of the relative displacements and the minimum chip thickness on the surface texture in shoulder milling. Materials 2023; 167661. https://doi.org/10.3390/ma16247661
8. Chatys R., Kłonica M., Blumbergs I. Analysis of fatigue and residual strength estimation of polymer matrix composites using the theory of the Markov chain method. Materials. 2025; 18: 1–17. https://doi.org/10.3390/ma18143229
9. Królikowski W. Polymer structural composites. Scientific Publishing PWN SA, Warsaw, 2012.
10. Wang, X.M., Zhang, L.C. An experimental investigation into the orthogonal cutting of unidirectional fibre reinforced plastics. Int. J. Mach. Tools Manuf. 2003; 43: 1015–1022. https://doi.org/10.1016/S0890-6955(03)00090-7
11. Slamani, M., Chatelain, J.-F. A review on the machining of polymer composites reinforced with carbon (CFRP), glass (GFRP), and natural fibers (NFRP). Discov. Mech. Eng. 2023; 2: 4. https://doi.org/10.1007/s44245-023-00011-w
12. Lakho D.A., Yao D., Cho K., Ishaq M., Wang Y. Study of the curing kinetics toward development of fast-curing epoxy resins. Polym.-Plast. Technol. Eng. 2017; 56: 161–170.
13. Korzekwa J., Bociąga E., Bochenek D. Investigation of selected polymer composite-aluminum oxide coating tribological systems. Materials 2020; 13(23). https://doi.org/10.3390/ma13235491
14. Bociaga E., Monika K., Kwiatkowski K. Analysis of structural changes in injection-molded parts due to cyclic loading. Advances in Polymer Technology, 2018; 37(6): 2134–2141; https://doi.org/10.1002/adv.21872
15. Zhang J., Xu Y. C., Huang P. Effect of cure cycle on curing process and hardness for epoxy resin, Polymer 2009; 3(9): 534–541. https://doi.org/10.3144/expresspolymlett.2009.67
16. Ren R., Chen P., Lu S., Xiong X., Liu S. The curing kinetics and thermal properties of epoxy resins cured by aromatic diamine with hetero-cyclic side chain structure. Thermochim. Acta 2014; 595: 22–27.
17. Skoczylas J., Kłonica M., Samborski S. A study on the FRP composite's matrix damage resistance by means of elastic wave propagation analysis. Composite Structures. 2022; 297: 1–21. https://doi.org/10.1016/j.compstruct.2022.115935
18. Wang, H., Sun, J., Zhang, D., Guo, K., Li, J. The effect of cutting temperature in milling of carbon fiber reinforced polymer composites. compos. Part A Appl. Sci. Manuf. 2016; 91: 380–387. https://doi.org/10.1016/j.compositesa.2016.10.025
19. Danish, M., Gupta, M.K., Rubaiee, S., Ahmed, A., Mahfouz, A., Jamil, M. Machinability investigations on CFRP composites: A comparison between sustainable cooling conditions. Int. J. Adv. Manuf. Technol. 2021; 114: 3201–3216. https://doi.org/10.1007/s00170-021-07073-8
20. Grzesik W., Attia H., Wegener K., Rech, J., Balazinski M. Intelligent methods for quantifying and determining friction in the cutting process – A review. Journal of Machine Engineering, 2026; 26: 36–50. https://doi.org/10.36897/jme/218157
21. Gühring Catalogue - Solid Carbide End Mills, Series 19992.
22. Piotrowski J.Zb., Orman Ł.J., Lucas X., Zender–Świercz E., Telejko M., Koruba D. Tests of thermal resistance of simulated walls with the reflective insulation, Proc. of Int. Conf. "Experimental Fluid Mechanics 2013", Czech Republic, EPJ Web of Conferences 2014; 67. https://doi.org/10.1051/epjconf/20146702095
23. Radek N., Konstanty J., Pietraszek J., Orman Ł.J., Szczepaniak M., Przestacki D. The effect of laser beam processing on the properties of WC-Co coatings deposited on steel, Materials 2021; 14: 538. https://doi.org/10.3390/ma14030538
24. Bronis M., Miko E., Nowakowski L., Bartoszuk M. A study of the kinematics system in drilling Inconel 718 for improving of hole quality in the aviation and space industries, Materials 2022; 15: 5500. https://doi.org/10.3390/ma15165500